



Feasibility of TEMPO-functionalized Imidazolium, Ammonium and Pyridinium Salts as Redox-Active Carriers in Ethaline Deep Eutectic Solvent for Energy Storage

| | |
|-------------------------------|---|
| Journal: | <i>Molecular Systems Design & Engineering</i> |
| Manuscript ID | ME-ART-04-2020-000038.R1 |
| Article Type: | Paper |
| Date Submitted by the Author: | 19-Jun-2020 |
| Complete List of Authors: | Chen, Brian; Case Western Reserve University Mitchell, Sarah; Texas A&M University System, Chemistry Sinclair, Nicholas; Case Western Reserve University, Chemical and Biomolecular Engineering Wainright, Jesse; Case Western Reserve University, Chemical and Biomecular Engineering Pentzer, Emily; Texas A&M University System, Chemistry, Materials Science and Engineering Gurkan, Burcu; Case Western Reserve University, Chemical and Biomolecular Engineering |
| | |

SCHOLARONE™
Manuscripts

We have designed molecular structures involving the nitroxyl radical to bring the capability of redox activity to ethaline deep eutectic solvent which is composed of choline chloride and ethylene glycol. Specifically, we show how the solubility of the charge carrier can be improved by modification of the structure with hydroxyl functionality as well as derivatization into salt. This strategy is ultimately expected to lead to increased energy density in energy storage systems. Furthermore, we investigate the impact of structure on transport properties and redox reversibility that are critical for redox flow battery technology. We discuss the opportunities and also the limitations of these solvent systems to help guide future studies in this field.

**Feasibility of TEMPO-functionalized Imidazolium, Ammonium and Pyridinium
Salts as Redox-Active Carriers in Ethaline Deep Eutectic Solvent for Energy
Storage**

Brian Chen,^{1,†} Sarah Mitchell,^{2,†} Nicholas Sinclair^{1,†}, Jesse Wainright^{1,*}, Emily Pentzer,^{2,*} Burcu
Gurkan^{1,*}

¹Department of Chemical Engineering Biomolecular Engineering, Case Western Reserve University, 10900 Euclid Avenue, Cleveland, Ohio 44106, United States

²Department of Chemistry, Department of Materials Science and Engineering, Texas A&M University, College Station, Texas 77840, United States

† These authors equally contributed

*Corresponding author

ABSTRACT

The discovery of electrolytes that have low vapor pressures and high solubility towards redox active species with an ability to undergo multiple electron transfer reactions is a challenge to realize in large-scale energy storage. Herein, we investigate the feasibility of (2,2,6,6-tetramethylpiperidin-1-yl)oxyl (TEMPO) derived halide salts as redox active species in ethaline (1:2 ethylene glycol:choline chloride), a deep eutectic solvent (DES). Hydrogen bonding and electrostatic interactions achieved by the functionalization of TEMPO are shown to improve solubility in ethaline. This is the first study evaluating the physical properties and electrochemical behavior of the newly synthesized TEMPO-salts in ethaline providing insight into the impact of chemical functionality on the utility of these redox active species in DESs.

INTRODUCTION

Deep eutectic solvents (DESs)¹ are comprised of a hydrogen bond donor (HBD) and hydrogen bond acceptor (HBA) whose mixture at the eutectic composition has a depressed melting point compared to the parent compounds and that of the ideal mixture expectation. DESs have low vapor pressures and the individual components are biodegradable and non-toxic, making them great candidates as a “greener” alternative to ionic liquids.^{1–4} Moreover, compared to ionic liquids (ILs), DESs are more easily prepared on large scales and are low-cost. Commonly reported HBAs are halide salts such as the quaternary ammonium-based choline chloride (ChCl).^{5,6} The HBD can be a variety of small molecules, ranging from alcohols^{7,8} to amines⁹ to acids.¹⁰ In a DES, the HBD and HBA form a hydrogen bond network that is believed to account for the depressed melting point.⁹ DESs are highly attractive due to tunable physico-chemical properties. The simplest route to tune the physical properties of a DES is to vary the HBD using the same HBA. This formulation produces a large number of DESs with a range of density, viscosity, conductivity and polarity.^{1,4,9,11,12} For example, Bahadori *et al.*¹³ reported physical properties and electrochemical stability of seven DESs formed between combinations of a HBA (choline chloride (ChCl) or *N,N*-diethylethanol ammonium chloride) and HBD (malonic acid, oxalic acid, triethanolamine, trifluoroacetamide, or Zn(NO₃) hexahydrate). Density and ionic conductivity measurements showed no trend dependent on the HBD identity, however both properties were temperature dependent. In contrast, the viscosity of the DES did depend on the identity of the HBD, with an amide HBD exhibiting the lowest viscosity, followed by the metal hydrate.

With many possibilities of HBA and HBD molecules and very limited design principles, it is difficult to determine a priori which of the HBA-HBD pairs and at which composition would actually result in a deep eutectic mixture. Recently, with the availability of new experimental density and vapor pressure data, it was possible to model DESs with Perturbed-Chain Statistical Associating Fluid Theory (PC-SAFT) to understand melting temperature¹⁴ and solubility of species such as water.¹⁵ Such modeling efforts will be beneficial to understand the physical phenomena in DESs as well as predicting the suitability of specific DESs for applications such as CO₂ capture,¹⁶ electrodeposition of metals,^{17,18} and separations.^{19–22} DESs have been advantageous in electrodeposition processes specifically for their ability to dissolve metal salts. DESs also have the potential to overcome solubility issues associated with traditional electrolytes adapted for redox flow batteries (RFBs), and thus could increase the energy density by dissolving appreciable amounts of redox active solutes.²³ Among the numerous DESs reported, ethaline (a 1:2 molar mixture of ChCl and ethylene glycol (EG)) has low viscosity, 36 cP at 25 °C.²⁴ For any flow process utilizing DESs, viscosity is an important property; therefore, ethaline may be of interest for RFBs. In RFBs, the electrochemical kinetics depend on the diffusion coefficient (apart from the electron transfer rate constant at the electrode) of the redox-active molecule, which is dependent on the viscosity of the electrolyte. Lloyd et al. reported the first all-copper RFB utilizing ethaline as the electrolyte with 94% charging/discharging efficiency, but only 52% energy efficiency (at 10 mA/cm² at 50 °C), a limitation they attributed to viscosity.²⁵ In a similar vein, Miller et al. studied the physical and electrochemical properties of solutions of ChCl and EG (including ethaline) containing FeCl₂ and FeCl₃. The authors pointed out the promising aspects of these systems for RFBs due to the high concentration of iron (6.3 M), large voltage window, and low volatility.²⁶

In a recent review on organic RFBs by Luo et al.,²⁷ several advantages of redox-active organic molecules over inorganics such as metal halides are discussed. In particular, organic redox active molecules are earth-abundant and low-cost, making them attractive as scalable systems, and are also synthetically tunable, and thus ideal to systematically understand how chemical structure relates to properties and performance. A common redox active organic molecule is 2,2,6,6-tetramethylpiperidin-1-yl)oxyl (TEMPO), a stable organic radical with a well-defined, single-electron redox reaction.^{28,29} Using cyclic voltammetry (CV), Nishide *et al.*²⁸ showed that in acetonitrile, TEMPO undergoes a reversible, single-electron redox reaction at a half-wave potential ($E_{1/2}$) of +0.63 V vs. Ag/AgCl. The authors identified that the anodic and cathodic peaks corresponded to the oxidation of the nitroxide radical to oxoammonium cation and subsequent reduction back to the nitroxide radical, using electron spin resonance spectroscopy (ESR) to elucidate the redox mechanism (ESR detected the disappearance and re-appearance of the unpaired electron). The separation between these two peaks was narrow ($\Delta E < 70$ mV) which is indicative of a reversible system.

Aside from Nishide's work demonstrating the redox behavior of TEMPO in acetonitrile, other investigations evaluated the effect of molecular structure on redox behavior of modified TEMPO derivatives for both aqueous³⁰⁻³² and non-aqueous electrolytes³³⁻³⁵. 4-hydroxy-TEMPO (4HT), for example, is a TEMPO derivative with a hydroxyl (-OH) functional group at the 4 position. 4HT has been reported to have appreciable solubility in an aqueous electrolyte (2.1 M in 0.5 M NaCl), suggesting that the -OH functional group on 4HT increases solubility.³⁰ In a report by Chang et al.,³¹ a TEMPO derivative modified with a 1-methyl-imidazolium chloride salt was studied using CV and its redox behavior was compared with 4HT in aqueous NaCl electrolyte solutions. The

half-cell potential, $E_{1/2}$, of 4HT was reported to be +0.56 V vs. Ag quasi-reference electrode (QRE) and the $E_{1/2}$ of the imidazolium-modified TEMPO was +0.71 V vs. Ag QRE. This study demonstrated that by chemically modifying the TEMPO unit, the redox potential for formation of the oxoammonium cation can be shifted. The authors attributed this change to the electron-withdrawing nature of the imidazolium unit. In a similar study by Janoschka *et al.*,³⁶ a TEMPO derivative bearing a trimethyl ammonium chloride functional group was studied using CV and compared with 4HT. The reported $E_{1/2}$ for the trimethyl ammonium-modified TEMPO derivative was +0.79 V vs. Ag/AgCl, which was more positive than 4HT at +0.64 V vs. Ag/AgCl in 0.1 M NaCl aqueous solution. Similar to the imidazolium-modified TEMPO, the trimethyl ammonium TEMPO derivative has a more positive redox potential, again attributed to the electron-withdrawing nature of the new functional group (trimethyl ammonium). The authors also noted a significant increase in solubility in the aqueous electrolyte upon functionalization: the maximum concentration for 4HT was 0.5 M and that of the trimethyl ammonium-modified TEMPO was 3.2 M. As such, modification of the chemical composition of the TEMPO unit influences both redox potentials and solubility in aqueous electrolytes; to date, the impact of chemical modification on solubility and redox activity of organic small molecules in DES electrolytes are unknown.

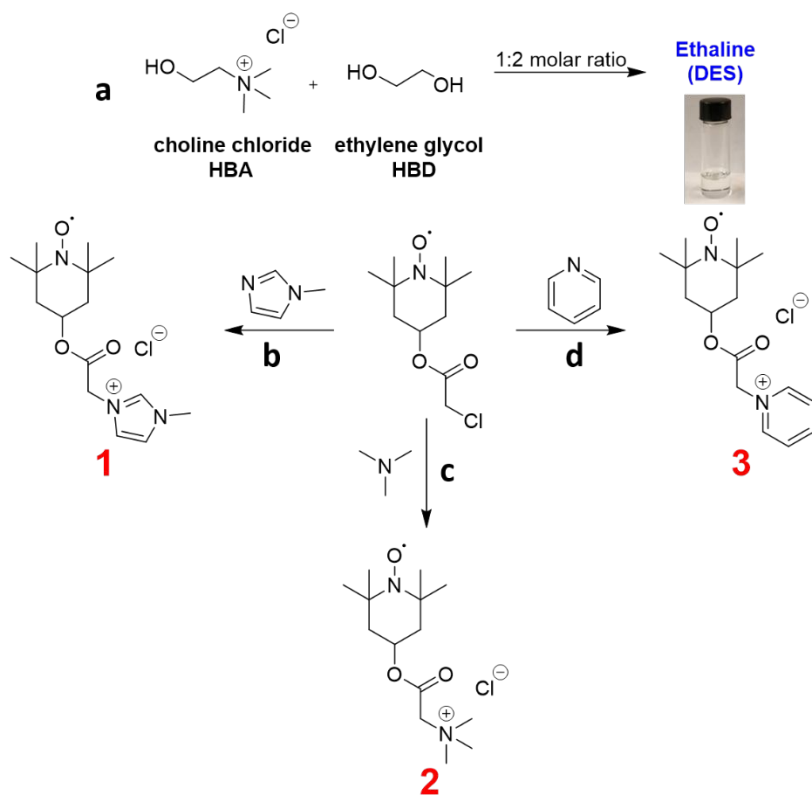
Herein, we discuss the physical properties, impact of structure on the solubility, impact of HBD on the stability, and electrochemical redox behavior of an all-organic redox active electrolyte containing TEMPO as the redox active unit in the DES ethaline, thus providing insight into the feasibility of such systems in RFBs. Specifically, we evaluate ethaline solutions of TEMPO, 4HT, and TEMPO modified with imidazolium, ammonium, and pyridinium chloride salts (referred to as **1**, **2**, and **3**, respectively). These newly formulated redox active DES solutions based on the TEMPO

unit and ethaline highlight the importance of solvation and the critical need for improved electrochemical stability in DESs for the next generation of large-scale energy storage systems.

RESULTS AND DISCUSSION

Synthesis of the modified TEMPO derivatives salts **1**, **2** and **3** is shown in **Scheme 1**. First, 4HT was converted to an α -chloro acetate intermediate by reaction with chloroacetic acid to form the ester. This intermediate was then converted to the imidazolium, ammonium, or pyridinium TEMPO-based salts by nucleophilic displacement of the chloride with *N*-methyl imidazole, trimethyl amine, and pyridine, respectively. The solubility limits of **1**, **2**, **3**, TEMPO, and 4HT in ethaline were determined using UV-Vis absorption spectroscopy (see **Figure S1** for details). The solubility limit of TEMPO (0.17 M) was significantly lower than that of 4HT (1.93 M) whereas the TEMPO salts had intermediate solubility, being more soluble than TEMPO and less soluble than 4HT. For the different cations, the solubility limit increased from trimethyl ammonium (1.35 M) > imidazolium (0.94 M) > pyridinium (0.85 M) for compounds **2**, **1**, and **3**, respectively (see **Table S1**). The specific advantage of the salts over 4HT is their potential to address the challenge of crossover of active redox active components through the separator membrane in RFBs. Functionalizing TEMPO with imidazolium, ammonium and pyrrolidinium salts introduces charge to the redox active specie while also increasing its molecular size; both strategies have been shown to suppress crossover compared to charge-neutral redox species in flow systems.^{27,36} To study the physical and electrochemical properties of TEMPO, 4HT, and the modified TEMPO derivatives in ethaline, three concentrations within the solubility limit of each compound were

studied. For comparisons to be made, similar concentrations were evaluated when available, and the water content for each system was determined prior to use (all <400 ppm, **Table S1**).



Scheme 1. Synthesis of ethaline and TEMPO derivatives (a) ethaline synthesis, (b) Compound **1**- synthesized in acetonitrile at 60°C for 48 hrs, (c) Compound **2**- synthesized in tetrahydrofuran at room temperature for 24 hrs, (d) Compound **3**- synthesized in acetonitrile at 60°C for 72 hrs.

The measured densities of ethaline solutions of TEMPO, 4HT, **1**, **2**, and **3** in the temperature range of 25 – 55 °C are shown in **Figure 1**. The incorporation of either TEMPO or 4HT led to decreased density as their concentration increased; this observation suggests an increase in the molar volume of the liquid. Specifically, in the case of 4HT (**Figure 1b**), considering its high solubility in ethaline, the hydrogen bonding network may be altered in a way that increases the molar

volume. This is opposite to what is generally expected from solutes with H-bonding ability, where increased H-bonding promotes an increase in density as a result of stronger intermolecular interactions.³⁷ These differences may be attributed to replacement of some of the H-bonds between ChCl and EG and between EG molecules, with H-bonds between ChCl and 4HT or 4HT and EG; thus, a rich H-bonding network in terms of liquid heterogeneity may be formed. In these micro environments, replacement of the more flexible aliphatic chains in ChCl and EG with the more rigid structure of 4HT can lead to an increase in the void size. On the contrary, the addition of TEMPO salts **1**, **2**, and **3** all led to an increase in density. This observation can possibly be explained by the occupation of the salts within the existing free volume of ethaline. Out of the three TEMPO salts studied, compound **2** has the least influence on density, as seen in **Figure 1d**, and it has the highest solubility. Compounds **1** and **3** both have aromatic groups that promote tighter packing, thus leading to higher densities in solution. Therefore, both aromaticity and increased Coulombic interactions result in larger entropic gain for **1** and **3** compared to the other solutes evaluated. For all systems studied, density decreased with increased temperature, following a linear trend (**Figure 1**); this is consistent with general trends seen for ILs and DESs. The linear fit parameters to express the temperature dependence of the measured densities can be found in **Table S2**.

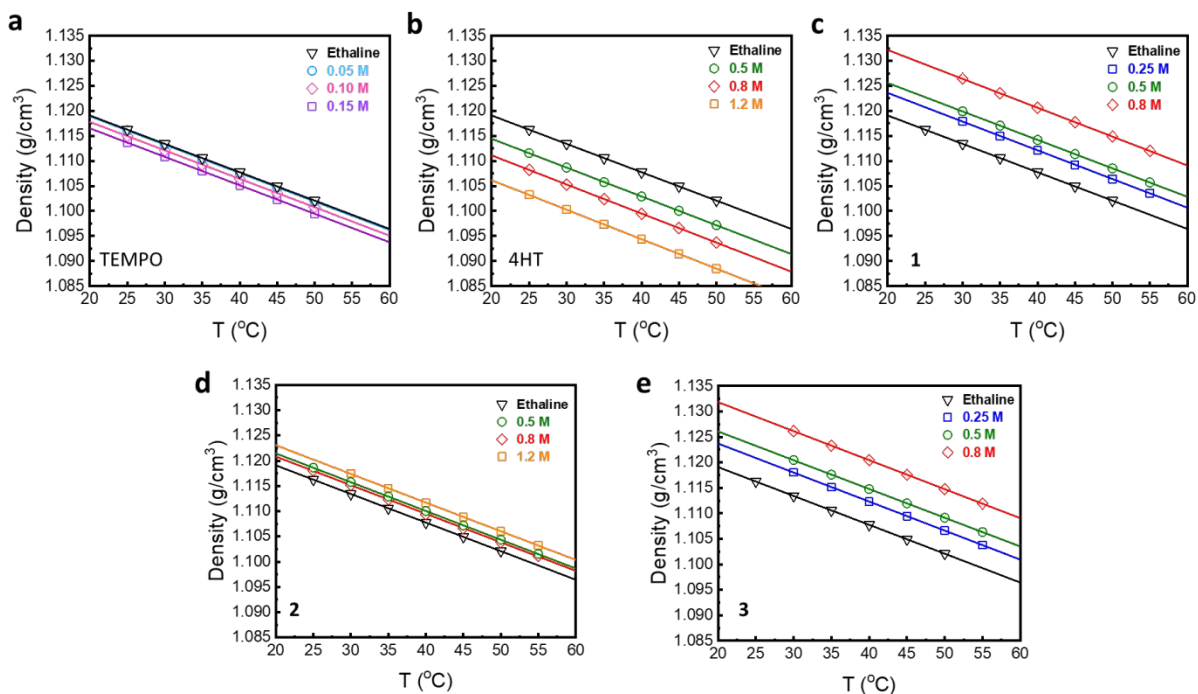


Figure 1. Temperature dependence of the measured densities for (a) TEMPO, (b) 4HT, (c) **1**, (d) **2**, and (e) **3** dissolved in ethaline.

The viscosities of ethaline solutions of TEMPO, 4HT, **1**, **2**, and **3** are shown in **Figure 2**. Unlike the different density trends of the neutral and salt solutes, viscosity increased irrespective of the identity of the redox active solute. While it is difficult to make comparisons between TEMPO and 4HT solutions due to the large differences in solubility, the $-OH$ in 4HT clearly promotes its integration to H-bonding network. What is interesting is that while the density decreases, viscosity increases with 4HT in ethaline (**Figure 2b**), despite the increased molar volume. This suggests that H-bond dynamics are slowed. Yet, the increase in viscosity with 4HT in ethaline is still small compared to the TEMPO salts. In the case of the TEMPO salts, **2** showed the lowest increase in viscosity (**Figure 2d**), whereas **1** and **3** had similarly increased viscosities, consistent with the observation in densities and attributed to the aromaticity of the cations. The increase in

measured viscosity for the TEMPO salts can be rationalized by the hole theory,³⁸ where the probability of finding holes of suitable radius for movement of ions and molecules in solution is hindered due to densified liquid structure.³⁹ The activation energies for all of the solutions obtained by the Arrhenius fits are about 30 kJ mol⁻¹, consistent with previous reports for ethaline,⁴⁰ with no sensitivity to the type of redox active solute in ethaline within the concentration ranges studied. The lines in **Figure 2** represent the Vogel-Tammann-Fulcher (VFT)⁴¹ fit to the measured viscosities as a function of temperature. DESs are known to be glass formers^{42–44} and their viscosity behavior is well represented by VFT;¹⁰ fitted parameters are given in **Table S3**.

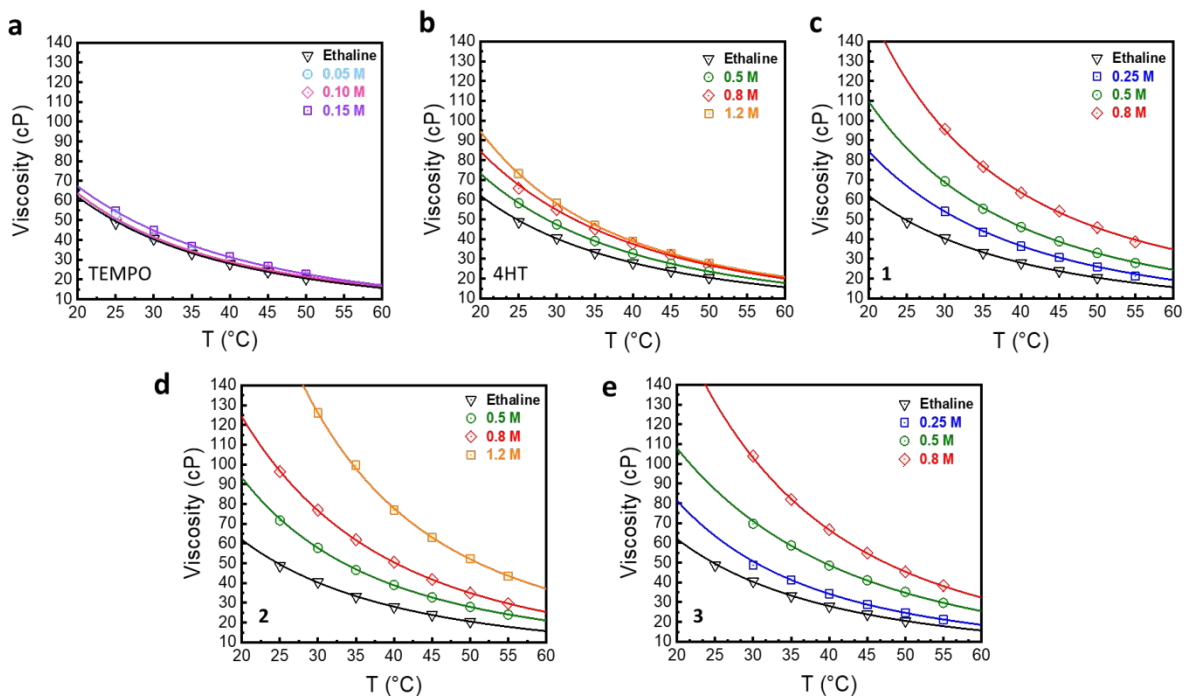


Figure 2. Temperature dependence of the measured viscosities for (a) TEMPO, (b) 4HT, (c) **1**, (d) **2**, and (e) **3** dissolved in ethaline.

Measured ionic conductivities for all solutions, shown in **Figure 3**, follow an opposite trend to the viscosities for the redox active solutes in ethaline: as the solute concentration is increased, conductivity decreased. Therefore, as the viscosity increased, conductivity decreased irrespective of whether the solute is neutral (TEMPO, 4HT) or charged (compounds **1**, **2**, and **3**). However, the inclusion of TEMPO salts resulted in lower conductivities compared to TEMPO and 4HT. In dilute or ideal electrolytes, increasing the salt content would increase conductivity.⁴⁵ With ethaline, increasing the salt content with the addition of **1**, **2** and **3**, resulted in stronger ionic associations (between the already present ChCl and the TEMPO salts), likely due to unavailability of the solvent molecules (EG) to dissociate the salt. The temperature dependence of conductivities can also be expressed by VFT as seen in solid lines in **Figure 3**. The fitted VFT parameters are given in **Table S4**.

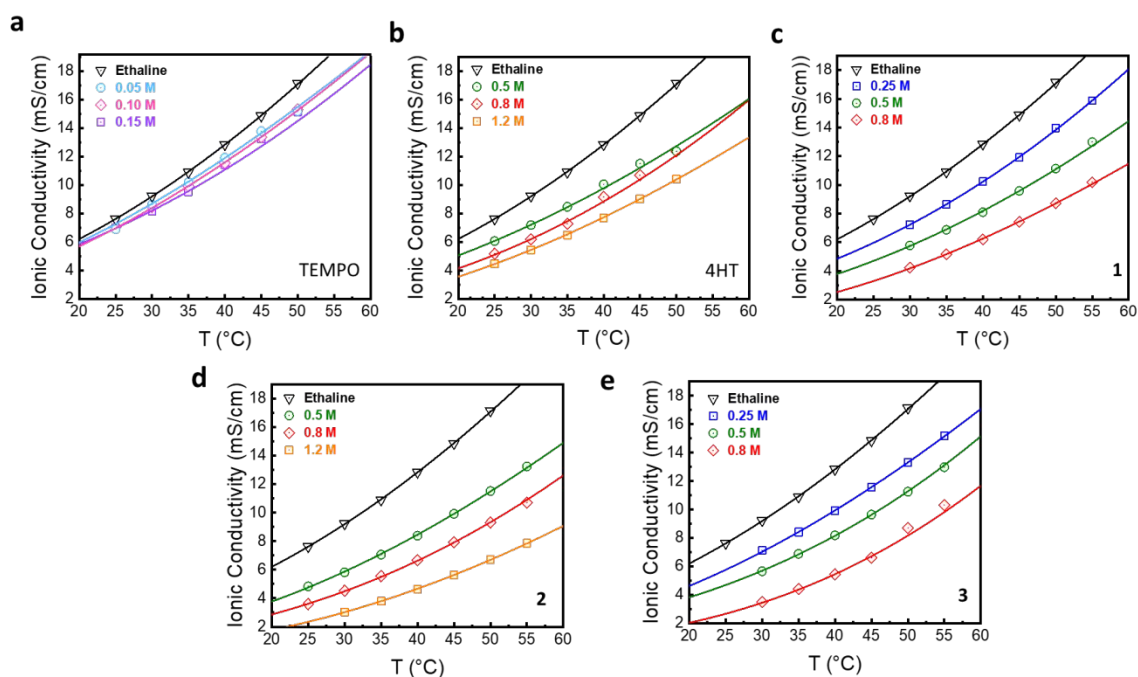


Figure 3. Temperature dependent of the measured ionic conductivities for (a) TEMPO, (b) 4HT, (c) **1**, (d) **2**, and (d) **3** dissolved in ethaline.

The redox behavior of 50 mM TEMPO in ethaline is shown in **Figure 4**. Two, single-electron reduction reactions are observed at +0.70 and -0.58 V vs. Ag/AgCl (denoted as E_1 and E_2). The first reduction (E_1) has its corresponding oxidation peak at +0.78 V, resulting in a half wave potential of +0.74 V vs. Ag/AgCl. The 80 mV separation of the reduction and oxidation reaction peaks and the roughly equal anodic and cathodic current densities suggest that this first redox reaction is reversible, at a first glance. This redox couple likely corresponds to the oxoammonium cation formation by the reduction of TEMPO, consistent with Nishide *et al.*'s²⁸ study of TEMPO in acetonitrile. Our own voltammetry study of TEMPO in acetonitrile confirms a +0.80 V vs. Ag/AgCl half wave potential (**Figure S2**), as reported in the literature. The negative shift by 60 mV in the redox potential of TEMPO to form an oxoammonium cation in ethaline as compared to acetonitrile can be attributed to the increased polarity of the solvent. This conjecture is supported by Manda *et al.*'s⁴⁶ report where the one-electron oxidation reaction of oxoammonium is shown to shift to more negative potentials as the solvent polarity increases.

Comparing the CV of TEMPO in ethaline to the CV in acetonitrile reveals an additional redox peak in ethaline at -0.58 V (E_2), which is due to the aminoxyl anion formation (see inset of **Figure 4**). This observation is consistent with TEMPO-based redox species reported in various electrolytes ranging from methanol to phosphate buffer upon cathodic polarization.^{35,47,48} The second electron transfer reaction (E_2) appears irreversible or quasi-reversible as evident from the reduced anodic current intensity on the oxidative scan and the broad oxidation peak.

Additionally, a third, very low intensity reduction peak at -0.07 V is observed after the 1st CV scan from the open circuit potential (OCP) to -1.5 V. Although the water content is low (140 ppm), hydroxyl formation with the aminoxyl anion following water electrolysis cannot be ruled out. It is also possible that the anion interacts with EG through H-bonding which can slow the redox reaction and result in the declination of its oxidation as seen from its wider potential with reduced peak current. Further electrokinetic experiments and careful analysis should be performed to verify this. However, this additional peak is consistently observed for all TEMPO species studied in ethaline, as seen in **Figure 5**.

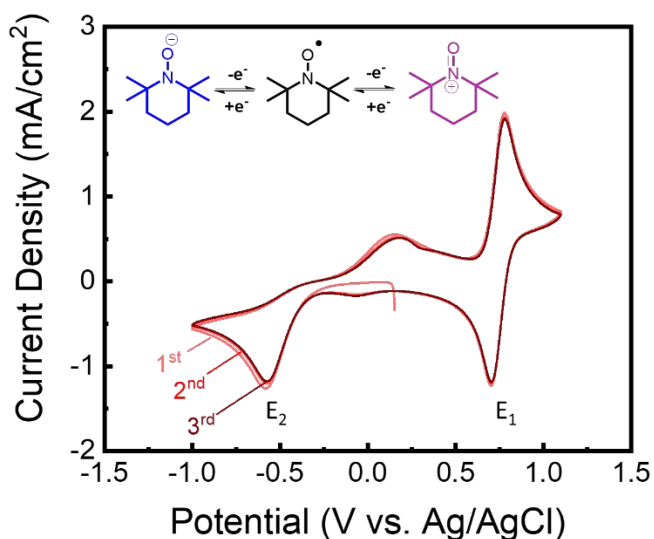


Figure 4. Cyclic voltammograms of 50 mM TEMPO in ethaline with 100 mV s⁻¹ scan rate; showing 3 cycles. CV performed with a glass carbon working, a coiled Pt wire counter around Ag/AgCl reference electrodes. Inset shows electrochemical reduction of TEMPO to oxoammonium (E₁) and oxidation of TEMPO to aminoxyl anion reduction (E₂).

Figure 5 shows the 1st, 2nd and 50th CV cycles for 4HT, **1**, **2**, and **3**. The two, single-electron redox reactions of TEMPO, E₁ and E₂, are observed for all derivatives. It should be noted that the solutions of compound **3** in ethaline had the lowest water contents (70-100 ppm) and the current intensity of the additional reduction in between E₁ and E₂ is negligible, as seen in **Figure 5d**. The pyridinium unit in **3** likely undergoes a reduction reaction where pyridinyl radical forms (**Scheme 2**) at -1.09 V,⁴⁹ more negative to the aminoxyl anion formation of TEMPO at -0.73 V. Due to its multi-electron redox capability, **3** could be an interesting compound for energy storage. However, the preliminary assessment of reversibility by the repeat of 50 CV cycles (**Figure 5d**) showed reduced reductive currents for both TEMPO and compound **3**, and very small oxidative currents of aminoxyl anion and pyridinyl radical upon cycling. On the other hand, 4HT, **1**, and **2** demonstrate greater redox stability over 50 cycles.

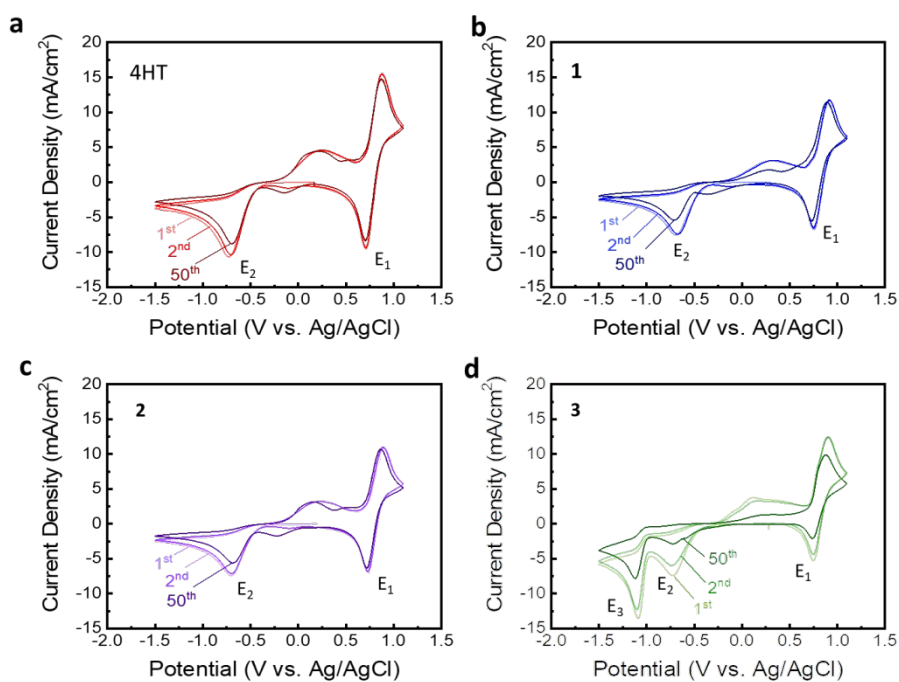
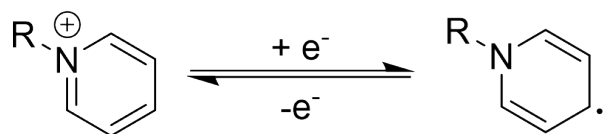


Figure 5. Cyclic voltammograms of (a) 4HT, (b) **1**, (c) **2**, (d) **3** at a concentration of 0.5 M for the 1st, 2nd, and 50th cycles. Scan rate was 100 mV s⁻¹. CV performed with a glass carbon working, a coiled Pt wire counter around Ag/AgCl reference electrodes.

Scheme 2. Reduction of pyridinium to pyridinyl radical



In ethaline, the reduction and oxidation peak separation of the reversible oxoammonium formation of 4HT is 170 mV, compared to 80 mV for TEMPO (**Table S5**). CVs with full potential range for electrochemical stability are shown in **Figure S3**. For the TEMPO salts **1**, **2**, and **3**, the peak separation is 160, 170 and 160 mV, respectively. Further, **1** and **3** demonstrate the greatest shift for the first reduction to oxoammonium at 0.76 and 0.75 V, respectively, compared to 0.70 V of TEMPO, 0.71 V of 4HT, and 0.72 V of **2**. These results indicate that substitution of TEMPO results in increased separation between the redox potentials. Furthermore, the aromatic cations of **1** and **3** create a more positive shift in the reduction potential of TEMPO compared to trimethyl ammonium **2** and neutral 4HT. The redox couple of TEMPO radical and oxoammonium cation was isolated in CV experiments by restricting the potential window to 0.5 - 1.1 V vs. Ag/AgCl, eliminating the quasi-reversible formation of the aminoxyl anion, and thus allowing the diffusion coefficients of the redox solutes to be estimated. **Figure S4** shows the plots of cathodic reduction current as a function of squared root of scan rate for compound **2** as an example. The linear fits in these plots, representing the Randles-Sevcik equation,^{50,51} suggest that solution species diffuse to the electrode surface. The estimated diffusion coefficients are summarized in **Table S5**. While

the absolute values of diffusivity may not be accurate due to the possible mass transport limitations, as the experiments were not performed with a micro-electrode, the trend follows the opposite of viscosities, where the 0.5 M 4HT in ethaline has the largest diffusion coefficient ($4 \times 10^{-8} \text{cm}^2 \text{s}^{-1}$) and the lowest viscosity. This is not surprising since 4HT has the smallest size and lacks charge to promote stronger associations with ethaline. Among the TEMPO salts, the diffusivity estimated for trimethyl ammonium compound **2** ($2 \times 10^{-8} \text{cm}^2 \text{s}^{-1}$) is twice the diffusivity of **1** and **3**. Clearly, the solvation of TEMPO-salts in ethaline has a significant impact on the transport properties that ultimately influence the redox behavior. Furthermore, solvation can influence redox kinetics and this should be further investigated when engineering these processes.

To better understand the redox behavior and study the stability and reversibility of these redox active species in ethaline, CV experiments were repeated with a Pt microelectrode following a flow-cell experiment. The detailed description of the flow cell can be found in our previous publications.^{52,53} These experiments specifically focused on 4HT which demonstrated the highest solubility and the lowest viscosity in ethaline. In order to lower the viscosity even further and eliminate significant mass transfer limitations in a flow cell, a mixture of ChCl:EG with 1:4 molar ratio was also tested as the solvent. The purpose of the flow cell experiment was to obtain known concentrations of the oxidized and reduced versions of 4HT and study the E_1 and E_2 redox reactions independently in a symmetric cell configuration. Symmetric cell characterization involves a single reservoir containing both oxidized and reduced forms of a single redox couple. This electrolyte is then pumped through flow battery hardware to create a 0V open circuit

potential “battery” in which the average resistance of the oxidation and reduction reactions of a single redox couple can be measured in a flow system separately from any second redox couple required for a viable flow battery. This method can also be used to investigate degradation effects of such as capacity fade over time since the electrolyte can be charged indefinitely with no change in state of charge (SOC).⁵⁴ First, 0.1 M 4HT in ChCl:EG (1:4) was placed in the positive half-cell and paired with 0.1 M FeCl₃ ChCl:EG (1:4) in the negative half-cell. Upon charging, the positive half-cell oxidizes 4HT to 4HT⁺ while the negative half-cell reduces Fe⁺³ to Fe⁺². To eliminate any ambiguity originating from the negative half-cell, Fe⁺³/Fe⁺² was chosen as a reliable and well-known redox couple. The concentrations of the various redox active species in the positive and negative electrolytes were evaluate at 50% SOC by performing CVs, as seen in **Figure 6a**. The positive half-cell electrolyte before charging is included for comparison (4HT 0% SOC).

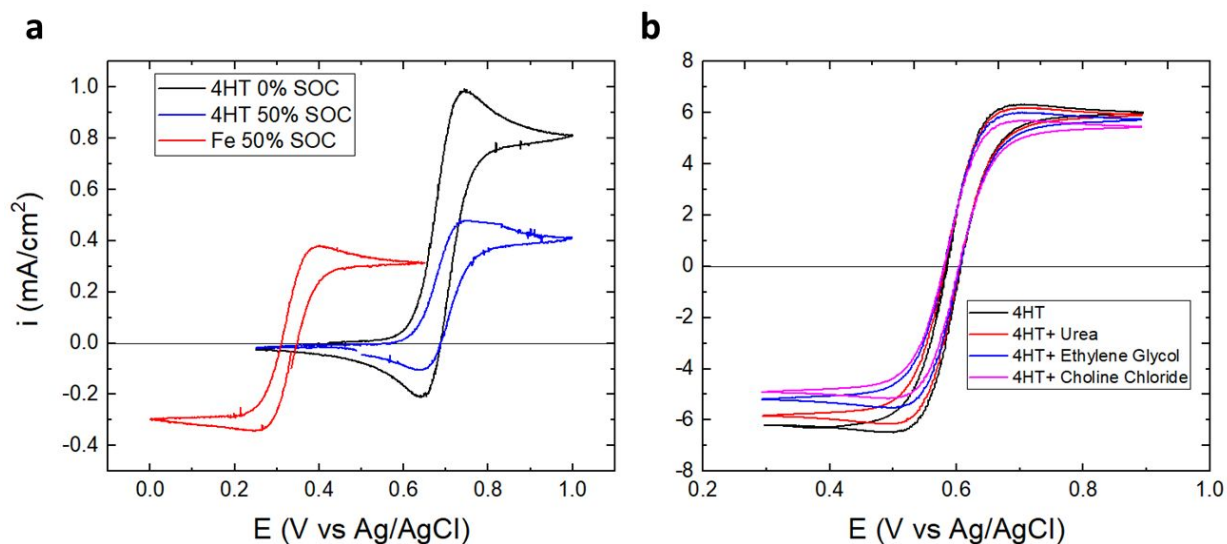


Figure 6. (a) Cyclic voltammograms of the positive and negative electrolytes of the flow cell following a 50% SOC for the initial electrolytes of 0.1M 4HT and 0.1M FeCl₃ in ChCl:EG (1:4), respectively. The positive half-cell electrolyte before charging is represented by the black curve

(4HT 0% SOC), the red curve is for $\text{Fe}^{3+}/\text{Fe}^{2+}$ at 50% SOC, and the blue curve is $4\text{HT}/4\text{HT}^+$ at 50% SOC. (b) Cyclic voltammogram of 0.1 M 4HT in 1 M KCl aqueous solution after being charged to 50% SOC (black curve). For comparison, this sample was dosed with EG, urea, or ChCl to a final concentration of 0.5 M in each. Experiments were performed with a 100 μm Pt disk electrode and at a sweep rate of 5 mV s^{-1} .

The data in **Figure 6a** correspond to steady-state currents as evident from the almost overlapping forward and reverse scans and are consistent with the micro-electrode equation (See eqn. 6 in Supporting Materials). For the negative electrolyte with $\text{Fe}^{3+}/\text{Fe}^{2+}$, the oxidation and reduction currents are equal indicating equal bulk concentrations of the oxidized (Fe^{3+}) and reduced (Fe^{2+}) species, consistent with our expectations from the amount of charge passed through the flow cell (50% SOC). However, the same is not true for the positive electrolyte with $4\text{HT}/4\text{HT}^+$. The oxidation current with a magnitude of 0.4 mA/cm^2 is obtained (4HT 50% SOC in **Figure 6a**, blue curve) with no corresponding steady-state reductive current. The similar behavior is observed for the positive electrolyte before charging (4HT 0% SOC in **Figure 6a**, black curve). Comparing the 0 and 50% SOC positive electrolyte, the decrease of the oxidation current by half from 0.8 to 0.4 mA/cm^2 confirms 50% SOC and proves that the 4HT oxidation reaction involves one electron. Similar experiments were repeated by replacing the negative electrolyte with 0.1 M 4HT in ChCl:EG with 1:4 and 1:2 molar ratios brought to 50 % SOC. With the $4\text{HT}/4\text{HT}^-$ in the negative side and $4\text{HT}/4\text{HT}^+$ on the positive side, the same behavior was observed for the $4\text{HT}/4\text{HT}^+$ couple while the $4\text{HT}/4\text{HT}^-$ showed reversibility consistent with one-electron transfer, but with sluggish kinetics (results not shown). The lack of a steady state reduction current in charged positive

reservoir suggests that the $4HT^+$ is either no longer electrochemically active or has undergone a subsequent reaction such that the concentration of $4HT^+$ in the charged electrolyte is essentially zero. This is unexpected based on the CVs shown in **Figure 5** and indicates that while at short time scales (minutes to 3 hours) $4HT^+$ appears stable in ethaline and electrochemically active, at longer times (>3 hours) $4HT^+$ undergoes a slow secondary reaction to form an electrochemically inactive compound.

To test our hypothesis and to understand the loss of active $4HT^+$, an experiment was performed in which a flow cell was used to charge a solution of 0.1 M 4HT in aqueous 1M KCl to 50% SOC., using of 0.1 M $K_3Fe(CN)_6$ as the negative electrolyte. The positive electrolyte was sampled and dosed with EG, urea, or ChCl individually to achieve a concentration of 0.5 M of each. The intent of these additions was to determine if the loss of electrochemical activity of the $4HT^+$ was due to the presence of common DES components (EG and urea are the HBDs in ethaline and reline respectively, and ChCl is the HBA salt in both cases). The CVs of these samples are shown in **Figure 6b**. It can be seen that the unaltered electrolyte (**Figure 6b**, black curve) is indeed at 50% SOC due to the equal magnitude of the oxidation and reduction currents (6 mA/cm^2) for 4HT and $4HT^+$, respectively. When the compounds added, the reduction current is decreased in comparison to a more or less stable oxidation current. Small changes to the oxidation current may be explained by an increase in the viscosity of the liquid and the dilution of the electrolyte with the addition of EG, urea, or ChCl. The addition of urea has a smaller effect on the reduction current than EG or ChCl, which both possess primary alcohol groups, in contrast to urea. It has been reported that $TEMPO^+$ can react with primary alcohols in aqueous systems.⁵⁵ Therefore, it

is possible that the alcohol group in EG gets oxidized to an aldehyde in the presence of TEMPO⁺ as suggested in **Scheme S1**. Before settling on this suggestion, further spectroscopic and quantitative studies are needed.

CONCLUSIONS

DESs have advantages for energy storage over aqueous electrolytes and those based on molecular solvents due primarily to their low vapor pressures and good solvent strength with capacity to increase the concentration of redox active species, and thus increase energy density. Here, we have reported the synthesis of three TEMPO salts, incorporated these redox active small molecules in the DES ethaline (1:2 ChCl:EG), and evaluated their impact on the physical properties and redox behavior, comparing to TEMPO and 4HT. We varied the identity of the cation covalently attached to TEMPO, studying the chloride salts of imidazolium, ammonium, and pyridinium functionalities (compounds **1**, **2**, and **3**, respectively). The TEMPO salts were more soluble in ethaline as compared to TEMPO, but less soluble than 4HT. Addition of TEMPO and 4HT to ethaline led to a decrease in density, whereas addition of **1**, **2** and **3** led to an increase in density. This can be attributed to differences in H-bonding, Coulombic interactions, and aromaticity of the cation structure. Addition of all compounds resulted in increased viscosity, with the TEMPO salts producing a larger increase than TEMPO or 4HT. The opposite trend was observed for ionic conductivity, where addition of all compounds to ethaline led to a decreased ionic conductivity. The redox behavior for each of the compounds in ethaline shows two, single-electron redox reactions corresponding to oxoammonium and aminoxyl anion formations.

Compound **3** also exhibits a third electron transfer reaction due to the pyridinium functionality. Compounds **1**, **2**, and 4HT demonstrate redox stability over 50 cycles at 100 mV/s, while TEMPO and compound **3** exhibit a reduced reductive current for all redox couples. The stability of the 4HT/4HT⁺ redox couple was further studied by flow cell experiments followed by voltammetry. The irreversibility of 4HT/4HT⁺ in the presence of ethaline is found to limit the potential utility of this specific system for RFBs. Nonetheless, this work illustrates that chemical modification of redox active organic molecules impacts both solubility in a DES electrolyte and their redox performance and physical properties of the solutions. Importantly, the trends reported here are in contrast to those identified for salt-modified TEMPO derivatives in aqueous electrolytes. Further research is needed to understand the molecular level interactions between the dissolved redox species and DESs, and to explain the macroscopic changes observed in physical properties as well as to guide molecular structures in these systems towards reversible redox reactions with improved stability and kinetics.

Conflicts of Interest

There are no conflicts to declare

Electronic Supplementary Information.

Materials and instrumentation, experimental methods, calibration curves, fit parameters to physical properties, voltammetry for electrochemical stability, electrochemical impedance spectroscopy, and spectroscopic confirmations of synthesized compounds.

AUTHOR INFORMATION

Corresponding Author

*E-mail: beg23@case.edu

*Email: emilypentzer@tamu.edu

*Email: jsw7@case.edu

ORCID

Brian Chen: 0000-0001-6496-6259

Sarah Mitchell: 0000-0002-0245-4589

Emily Pentzer: 0000-0003-4269-2641

Burcu Gurkan: 0000-0003-4886-3350

Jesse Wainright: 0000-0001-7902-7238

Acknowledgements

Authors would like to thank Robert Savinell and Rohan Akolkar on many useful discussions related to the electrochemical characterizations. This work was funded by Breakthrough Electrolytes for Energy Storage (BEES) -an Energy Frontier Research Center funded by the U.S. Department of Energy, Office of Science, Basic Energy Sciences under Award # DE-SC0019409.

REFERENCES

- (1) Smith, E. L.; Abbott, A. P.; Ryder, K. S. Deep Eutectic Solvents (DESS) and Their Applications. *Chem. Rev.* **2014**, *114* (21), 11060–11082.
- (2) Hayyan, M.; Ali, M.; Hayyan, A.; Al-saadi, M. A.; Alnashef, I. M.; Mirghani, M. E. S.; Kola, O. Are Deep Eutectic Solvents Benign or Toxic ? *Chemosphere* **2013**, *90* (7), 2193–2195.
- (3) Haerens, K.; Matthijs, E.; Chmielarz, A.; Bruggen, B. Van Der. The Use of Ionic Liquids Based on Choline Chloride for Metal Deposition : A Green Alternative ? *J. Environ. Manage.* **2009**, *90* (11), 3245–3252.
- (4) Zhang, Q.; Vigier, K. D. O.; Royer, S.; Jerome, F. Deep Eutectic Solvents: Syntheses, Properties and Applications. *Chem. Soc. Rev.* **2012**, *41*, 7108–7146.
- (5) Khalid, M.; Hayyan, M.; Abdulhakim, M.; Akib, S. Glycerol-Based Deep Eutectic Solvents: Physical Properties. *J. Mol. Liq.* **2016**, *215*, 98–103.
- (6) Ibrahim, R. K.; Hayyan, M.; Alsaadi, M. A.; Ibrahim, S.; Hayyan, A.; Hashim, M. A. Diethylene Glycol Based Deep Eutectic Solvents and Their Physical Properties. *Stud. Univ. Babeş-Bolyai Chem.* **2017**, *62* (4), 433–450.
- (7) Constantin, V.; Adya, A. K.; Popescu, A. M. Density, Transport Properties and Electrochemical Potential Windows for the 2-Hydroxy-N,N,N-Trimethylethanaminium Chlorides Based Ionic Liquids at Several Temperatures. *Fluid Phase Equilib.* **2015**, *395*, 58–66.
- (8) Yadav, A.; Kar, J. R.; Verma, M.; Naqvi, S.; Pandey, S. Densities of Aqueous Mixtures of (Choline Chloride + Ethylene Glycol) and (Choline Chloride + Malonic Acid) Deep Eutectic Solvents in Temperature Range 283.15–363.15 K. *Thermochim. Acta* **2015**, *600*, 95–101.

- (9) Abbott, A. P.; Capper, G.; Davies, D. L.; Rasheed, R. K.; Tambyrajah, V. Novel Solvent Properties of Choline Chloride / Urea Mixtures. *Chem. Commun.* **2003**, 70–71.
- (10) Sas, O. G.; Fidalgo, R.; Domínguez, I.; Macedo, E. A.; González, B. Physical Properties of the Pure Deep Eutectic Solvent, [ChCl]:[Lev] (1:2) DES, and Its Binary Mixtures with Alcohols. *J. Chem. Eng. Data* **2016**, *61* (12), 4191–4202.
- (11) Abbott, A. P.; Boothby, D.; Capper, G.; Davies, D. L.; Rasheed, R. K. Deep Eutectic Solvents Formed between Choline Chloride and Carboxylic Acids : Versatile Alternatives to Ionic Liquids. *J. Am. Chem. Soc.* **2004**, *126* (9), 9142–9147.
- (12) Kareem, M. A.; Mjalli, F. S.; Hashim, M. A.; Alnashef, I. M. Phosphonium-Based Ionic Liquids Analogues and Their Physical Properties. *J. Chem. Eng. Data* **2010**, *55*, 4632–4637.
- (13) Bahadori, L.; Chakrabarti, M. H.; Mjalli, F. S.; Alnashef, I. M.; Manan, N. S. A.; Hashim, M. A. Physicochemical Properties of Ammonium-Based Deep Eutectic Solvents and Their Electrochemical Evaluation Using Organometallic Reference Redox Systems. *Electrochim. Acta* **2013**, *113*, 205–211.
- (14) Pontes, P. V. A.; Crespo, E. A.; Martins, M. A. R.; Silva, L. P.; Neves, C. M. S. S.; Maximo, G. J.; Hubinger, M. D.; Batista, E. A. C.; Pinho, S. P.; Coutinho, J. A. P.; Sadowski, G.; Held, C. Measurement and PC-SAFT Modeling of Solid-Liquid Equilibrium of Deep Eutectic Solvents of Quaternary Ammonium Chlorides and Carboxylic Acids. *Fluid Phase Equilib.* **2017**, *448*, 69–80.
- (15) Dietz, C. H. J. T.; Erve, A.; Kroon, M. C.; van Sint Annaland, M.; Gallucci, F.; Held, C. Thermodynamic Properties of Hydrophobic Deep Eutectic Solvents and Solubility of Water and HMF in Them: Measurements and PC-SAFT Modeling. *Fluid Phase Equilib.* **2019**, *489*, 75–82.
- (16) Zhang, Y.; Ji, X.; Lu, X. Choline-Based Deep Eutectic Solvents for CO₂ Separation: Review and

- Thermodynamic Analysis. *Renew. Sustain. Energy Rev.* **2018**, *97* (July), 436–455.
- (17) A. Popescu, V. Constantin, A. Cojocaru, M. O. Electrochemical Behaviour of Copper (II) Chloride in Choline Chloride-Urea Deep Eutectic Solvent. *Rev. Chim.* **2011**, *62* (2), 206–211.
- (18) Shen, D.; Steinberg, K.; Akolkar, R. Avoiding Pitfalls in the Determination of Reliable Electrochemical Kinetics Parameters for the $\text{Cu}^{2+} \rightarrow \text{Cu}^{1+}$ Reduction Reaction in Deep Eutectic Solvents. *J. Electrochem. Soc.* **2018**, *165* (14), E808–E815.
- (19) Sas, O. G.; Castro, M.; Domínguez, Á.; González, B. Removing Phenolic Pollutants Using Deep Eutectic Solvents. *Sep. Purif. Technol.* **2019**, *227* (June), 115703.
- (20) Shahbaz, K.; Mjalli, F.S.; Hashim, M.A.; Alnashef, I. M. Using Deep Eutectic Solvents for the Removal of Glycerol from Palm Oil-Based Biodiesel. *J. Appl. Sci.* **2010**, *10* (24), 3349–3354.
- (21) Liu, X.; Xu, D.; Diao, B.; Zhang, L.; Gao, J.; Liu, D.; Wang, Y. Choline Chloride Based Deep Eutectic Solvents Selection and Liquid-Liquid Equilibrium for Separation of Dimethyl Carbonate and Ethanol. *J. Mol. Liq.* **2019**, *275*, 347–353.
- (22) Verevkin, S. P.; Sazonova, A. Y.; Frolkova, A. K.; Zaitsau, D. H.; Prikhodko, I. V.; Held, C. Separation Performance of BioRenewable Deep Eutectic Solvents. *Ind. Eng. Chem. Res.* **2015**, *54* (13), 3498–3504.
- (23) Chakrabarti, M.; Mjalli, F.; AlNashef, I.; Hashim, M. A.; Hussain, M. A.; Bahadori, L.; Low, C. Prospects of Applying Ionic Liquids and Deep Eutectic Solvents for Renewable Energy Storage by Means of Redox Flow Batteries. *Renew. Sustain. Energy Rev.* **2014**, *30*, 254–270.
- (24) Abbott, A. P.; Harris, R. C.; Ryder, K. S. Application of Hole Theory to Define Ionic Liquids by Their Transport Properties. *J. Phys. Chem. B* **2007**, *111*, 4910–4913.

- (25) Lloyd, D.; Vainikka, T.; Kontturi, K. The Development of an All Copper Hybrid Redox Flow Battery Using Deep Eutectic Solvents. *Electrochim. Acta* **2013**, *100*, 18–23.
- (26) Miller, M. A.; Wainright, J. S.; Savinell, R. F. Communication — Iron Ionic Liquid Electrolytes for Redox Flow Battery Applications. *J. Electrochem. Soc.* **2016**, *163* (3), 578–579.
- (27) Luo, J.; Hu, B.; Hu, M.; Zhao, Y.; Liu, L. Status and Prospects of Organic Redox Flow Batteries toward Sustainable Energy Storage. *ACS Energy Lett.* **2019**, *4*, 2220–2240.
- (28) Nishide, H.; Iwasa, S.; Pu, Y. J.; Suga, T.; Nakahara, K.; Satoh, M. Organic Radical Battery: Nitroxide Polymers as a Cathode-Active Material. *Electrochim. Acta* **2004**, *50* (2-3 SPEC. ISS.), 827–831.
- (29) Winsberg, J.; Hagemann, T.; Janoschka, T.; Hager, M. D.; Schubert, U. S. Redox-Flow Batteries : From Metals to Organic Redox- Active Materials. *Angew. Chemie - Int. Ed.* **2017**, *56*, 686–711.
- (30) Liu, T.; Wei, X.; Nie, Z.; Sprenkle, V.; Wang, W. A Total Organic Aqueous Redox Flow Battery Employing a Low Cost and Sustainable Methyl Viologen Anolyte and 4-HO-TEMPO Catholyte. *Adv. Energy Mater.* **2016**, *6*.
- (31) Chang, Z.; Henkensmeier, D.; Chen, R. Shifting Redox Potential of Nitroxyl Radical by Introducing an Imidazolium Substituent and Its Use in Aqueous Flow Batteries. *J. Power Sources* **2019**, *418* (February), 11–16.
- (32) Winsberg, J.; Stolze, C.; Schwenke, A.; Muench, S.; Hager, M. D.; Schubert, U. S. Aqueous 2,2,6,6-Tetramethylpiperidine-N-Oxyl Catholytes for a High-Capacity and High Current Density Oxygen-Insensitive Hybrid-Flow Battery. *ACS Energy Lett.* **2017**, *2* (2), 411–416.
- (33) Takechi, K.; Kato, Y.; Hase, Y. A Highly Concentrated Catholyte Based on a Solvate Ionic Liquid for Rechargeable Flow Batteries. *Adv. Mater.* **2015**, *27* (15), 2501–2506.

- (34) Li, Z.; Li, S.; Liu, S.; Huang, K.; Fang, D.; Wang, F.; Peng, S. Electrochemical Properties of an All-Organic Redox Flow Battery Using 2,2,6,6-Tetramethyl-1-Piperidinyloxy and N-Methylphthalimide. *Electrochem. Solid-State Lett.* **2011**, *14* (12), A171.
- (35) Park, S. K.; Shim, J.; Yang, J. H.; Shin, K. H.; Jin, C. S.; Lee, B. S.; Lee, Y. S.; Jeon, J. D. Electrochemical Properties of a Non-Aqueous Redox Battery with All-Organic Redox Couples. *Electrochem. commun.* **2015**, *59*, 68–71.
- (36) Janoschka, T.; Martin, N.; Hager, M. D.; Schubert, U. S. An Aqueous Redox-Flow Battery with High Capacity and Power: The TEMPTMA/MV System. *Angew. Chemie - Int. Ed.* **2016**, *55*, 14427–14430.
- (37) Ozturk, B.; Parkinson, C.; Gonzalez-miquel, M. Separation and Purification Technology Extraction of Polyphenolic Antioxidants from Orange Peel Waste Using Deep Eutectic Solvents. *Sep. Purif. Technol.* **2018**, *206* (March), 1–13.
- (38) Abbott, A. P. Application of Hole Theory to the Viscosity of Ionic and Molecular Liquids. *ChemPhysChem* **2004**, *5* (8), 1242–1246.
- (39) Cardellini, F.; Germani, R.; Cardinali, G.; Corte, L.; Roscini, L.; Spreti, N.; Tiecco, M. Room Temperature Deep Eutectic Solvents of (1S)-(+)-10-Camphorsulfonic Acid and Sulfobetaines: Hydrogen Bond-Based Mixtures with Low Ionicity and Structure-Dependent Toxicity. *RSC Adv.* **2015**, *5* (40), 31772–31786.
- (40) Troter, D. Z.; Todorović, Z. B.; Đokić-Stojanović, D. R.; Đordević, B. S.; Todorović, V. M.; Konstantinović, S. S.; Veljković, V. B. The Physicochemical and Thermodynamic Properties of the Choline Chloride-Based Deep Eutectic Solvents. *J. Serbian Chem. Soc.* **2017**, *82* (9), 1039–1052.
- (41) Fulcher, G. S. Analysis of Recent Measurements of the Viscosity of Glasses. *J. Am. Ceram. Soc.*

- 1925**, 75 (5), 1043–1055.
- (42) Sánchez, P. B.; González, B.; Salgado, J.; José Parajó, J.; Domínguez, Á. Physical Properties of Seven Deep Eutectic Solvents Based on L-Proline or Betaine. *J. Chem. Thermodyn.* **2019**, *131*, 517–523.
- (43) Wang, J.; Baker, S. N. Pyrrolidinium Salt Based Binary and Ternary Deep Eutectic Solvents: Green Preparations and Physiochemical Property Characterizations. *Green Process. Synth.* **2018**, *7* (4), 353–359.
- (44) Kadhom, M. A.; Abdullah, G. H.; Al-Bayati, N. Studying Two Series of Ternary Deep Eutectic Solvents (Choline Chloride–Urea–Glycerol) and (Choline Chloride–Malic Acid–Glycerol), Synthesis and Characterizations. *Arab. J. Sci. Eng.* **2017**, *42* (4), 1579–1589.
- (45) Reber, D.; Figi, R.; Kühnel, R. S.; Battaglia, C. Stability of Aqueous Electrolytes Based on LiFSI and NaFSI. *Electrochim. Acta* **2019**, *321*, 134644.
- (46) Manda, S.; Nakanishi, I.; Ohkubo, K.; Kawashima, T.; Matsumoto, K. I.; Ozawa, T.; Fukuzumi, S.; Ikota, N.; Anzai, K. Effect of Solvent Polarity on the One-Electron Oxidation of Cyclic Nitroxyl Radicals. *Chem. Lett.* **2007**, *36* (7), 914–915.
- (47) Manda, S.; Nakanishi, I.; Ohkubo, K.; Yakumar, H.; Matsumoto, K. I.; Ozawa, T.; Ikota, N.; Fukuzumi, S.; Anzai, K. Nitroxyl Radicals: Electrochemical Redox Behaviour and Structure-Activity Relationships. *Org. Biomol. Chem.* **2007**, *5* (24), 3951–3955.
- (48) Stoyanovsky, A. D.; Stoyanovsky, D. A. 1-Oxo-2,2,6,6-Tetramethylpiperidinium Bromide Converts α -H N,N-Dialkylhydroxylamines to Nitrones via a Two-Electron Oxidation Mechanism. *Sci. Rep.* **2018**, *8* (May), 15323.

- (49) Lucio, A. J.; Shaw, S. K. Pyridine and Pyridinium Electrochemistry on Polycrystalline Gold Electrodes and Implications for CO₂ Reduction. *J. Phys. Chem. C* **2015**, *119* (22), 12523–12530.
- (50) Randles, J. E. B. A Cathode Ray Polarograph. The Current-Voltage Curves. *Trans. Faraday Soc.* **1948**, *13*, 327–338.
- (51) Ševčík, A. Oscillographic Polarography with Periodical Triangular Voltage. *Collect. Czechoslov. Chem. Commun.* **1948**, *13*, 349–377.
- (52) Escalante-García, I. L.; Wainright, J. S.; Thompson, L. T.; Savinell, R. F. Performance of a Non-Aqueous Vanadium Acetylacetonate Prototype Redox Flow Battery: Examination of Separators and Capacity Decay. *J. Electrochem. Soc.* **2015**, *162* (3), A363–A372.
- (53) Hoyt, N. C.; Hawthorne, K. L.; Savinell, R. F.; Wainright, J. S. Plating Utilization of Carbon Felt in a Hybrid Flow Battery. *J. Electrochem. Soc.* **2016**, *163* (1), A5041–A5048.
- (54) Cazot, M.; Maranzana, G.; Dillet, J.; Beille, F.; Godet-Bar, T.; Didierjean, S. Symmetric-Cell Characterization of the Redox Flow Battery System: Application to the Detection of Degradations. *Electrochim. Acta* **2019**, *321*, 134705.
- (55) Angelin, M.; Hermansson, M.; Dong, H.; Ramstrom, O. Direct, Mild, and Selective Synthesis of Unprotected Dialdo-Glycosides. *European J. Org. Chem.* **2006**, No. 19, 4323–4326.

Design and considerations for all organic, redox-active, deep eutectic solvents for energy storage

